J Therm Anal Calorim (2013) 111:1351–1355
DOI 10.1007/s10973-012-2507-z

High-density nanoparticle ceramic bodies

A study of heating rates in the sinterization of Gadolinium-doped Ceria

Mario J. Godinho · Caue Ribeiro · Rosana F. Gonçalves · Elson Longo · Edson R. Leite

Received: 24 February 2012 / Accepted: 18 May 2012 / Published online: 3 July 2012

Abstract An investigation on the sinterization of Gd: CeO_2 ($Ce_{0.85}Gd_{0.15}O_{1.9-\delta}$ ceramic system) 3–10 nm nanoparticles in pressed bodies was done. The heating rate was taken as a key parameter and two competing sinterization processes were identified, associated with different diffusional mechanisms. Using heating rates of 113 °C min^{-1}, a high-final density (98 % of the theoretical) was obtained by superposing the two aforementioned mechanisms, resulting in a homogeneous microstructure at lower temperatures.

Keywords Sintering · Nanocrystalline materials · Powder consolidation · Sol–gel · Fuel cell materials

Introduction

Ceria compounds have been widely used as solid electrolyte [1–3] and catalysts [4]. In the fabrication of electrolytes (i.e., O^{2-} permeable electrolytes in solid oxide fuel cells), high-final densities of the sintered bodies are particularly desirable to improve the efficiency of energy conversion by preventing the permeation of other gases [5, 6].

Nanoparticles from soft-chemical synthesis are good candidates to obtain highly homogeneous stoichiometrically-controlled compounds. Several methods of synthesization, such as OPM [7], microemulsion [8], polymeric precursors [9], precipitation [10–13], partial oxalates [14], controlled hydrolysis [15], etc., are efficient to obtain such doped materials. In principle, the high-surface area of nanoparticles should favor the sinterization process through the high-boundary mobility associated with those areas [16]. In fact, nanoparticles with an average size of about 10 nm have a surface area of about 100 m^2/g, indicating high-accumulated energy at the grain boundaries [6]. Moreover, smaller grain sizes should result in improved mechanical properties and superplastic net-shape forming behavior. The consolidation of loosely agglomerated nanoparticles (smaller than 10 nm) of ceramic materials is expected to result in significant payoffs.

However, nanoparticles generally have near-monodisperse distributions and the poor packing associated with these cases implies low green densities and a large fraction of voids, which hamper the densification process [16]. In addition, the frequent occurrence of agglomerations can lead to abnormal grain growth, impairing the properties of the final body [17]. Several factors such as Van der Waals forces, capillarity, rugosity, particle shape, etc. interfere in a powder's dispersion [18, 19]. In fact, controlling agglomeration is still difficult, particularly in the synthesization of large amounts of nanometric powders. Therefore, an alternative is to investigate the behavior of green bodies obtained from agglomerated powders (powders with uncontrolled dispersion sizes) during their synthesis to

M. J. Godinho (✉) · R. F. Gonçalves
Departamento de Química, Universidade Federal de Goias, Campus Catalao, Catalao, GO 75704-020, Brazil
e-mail: godinho.mj.ufg@gmail.com

C. Ribeiro
EMBRAPA Instrumentacao, Rua XV de Novembro, 1452, CP 741, São Carlos, SP 13560-970, Brazil

E. Longo
Instituto de Química, LIEC—Universidade Estadual Paulista, Rua Francisco Degni, s/n, Araraquara, SP 14800-900, Brazil

E. R. Leite
Departamento de Química, LIEC—Universidade Federal de São Carlos, Rod. Washington Luiz, Km 235, São Carlos, SP 13565-905, Brazil

control the processing parameters as a way to obtain high-density ceramics. In the final process of an agglomerated $NaNbO_3$ powder, Leite et al. [20] achieved good densification values by controlling the heating rates in pressed bodies; however, to the best of our knowledge, this alternative has been little investigated in other systems.

The main goal of this study is to demonstrate a sintering process in which the densification of agglomerates can be controlled, favoring mass transport between individual Gd:CeO_2 nanoparticles. The results of this study may lead to a deeper understanding of nanoparticle densification and to new methodologies for the production of nanostructured highly densified ceramics.

Experimental

The detailed experimental routine for the synthesis is described elsewhere [10]. Solutions were prepared of 0.1 M of hexahydrate cerium(III) nitrate—$Ce(NO_3)_3{\cdot}6H_2O$ 99.9 % (Aldrich) dissolved in different solvents. Gadolinium(III) oxide—Gd_2O_3 99.9 % (Aldrich), dissolved in a minimum amount of nitric acid, was then added to the solution. Ammonium hydroxide was added to this mixture a drop at a time (under stirring) to complete the precipitation under controlled pH = 10, resulting in the formation of a white gel. This gel was then collected by vacuum filtration and washed to completely remove all the ammonium nitrate formed. X-ray diffraction showed a single-phase $Ce_{0.85}Gd_{0.15}O_{1.9-\delta}$ powder. Particle characterization by surface area measurements using the Brunauer–Emmett–Teller method revealed surface areas of about 114 $m^2\ g^{-1}$, indicating a highly reactive powder. TEM measurements confirmed the average particle size was 5.5 nm, as reported in [10].

Samples were formed into pellets (Ø = 9 mm, h = 4 mm) and pressed isostatically at 100 MPa, resulting in green densities close to 54 % of the theoretical density. Sintering was carried out in a dilatometer at temperatures of up to 1,550 °C (Netzsch 402, Germany), using several constant heating rates (2–40 °C min^{-1}), and in a homemade microwave furnace at a heating rate of 113 °C min^{-1}, in a similar experimental setup as described by Harabi et al. [21]. The morphology and fired density of the final samples were analyzed by scanning electron microscopy (SEM–FEG, ZEISS model-SUPRA 35).

Results and discussion

Figure 1 depicts the dilatometric profile of the samples sintered at 10 °C/min. The dilatometric curves showed two sintering stages at 850 °C (P_1) and 1,450 °C (P_2), indicated by the derivative curve. Based on similar studies of $NaNbO_3$ processing, Leite et al. [20] and Nobre et al. [22] proposed that the first stage is related to the agglomerate's sinterization and the second to dispersed particles, attributing them to advanced sintering mechanisms [23, 24]. The unambiguous determination of a sintering mechanism is complicated by the possible effects of combined mechanisms and, in the case of diffusion, by the similarity of the time dependence of surface and volume diffusion [25].

In this context, Fig. 2a shows dilatometric curves obtained at different heating rates. The sintering mechanisms are clearly dependent on the heating rate, showing a shift to higher temperatures in the first mechanism and to lower temperatures in the second, as indicated in Fig. 2b. Correlating the first peak to the sintering of agglomerates, it can be stated that this phenomenon is related to diffusion-activated sintering, in this case due to the fact that the particle growth may occur mainly by boundary diffusion of the contact particles. This process involves a low activation energy, which is confirmed by the low-activation temperatures observed; however, the process is essentially slow, since it depends on the movement of ions / atoms in the already formed lattices.

According to the temperatures observed, the second peak may be correlated with diffusion into the pre-sintered grains, re-shaping the structure, and then implying in densification. In fact, this mechanism is presumably the only path for growth in these conditions since no formation of liquid phase was observed. Although this supposition may be true, this second peak is still under investigation and its origin remains unclear. The high-heating rates may have favored the process through a kinetic effect, i.e., rapid diffusion of minor particles. In fact, variations in the transition temperatures of nanoparticles were investigated in detail, revealing, for instance, significant decreases in the melting point of Na and CdS [26, 27].

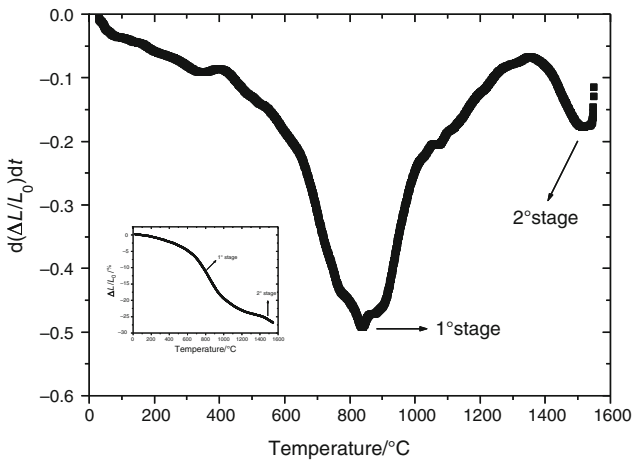

Fig. 1 Dilatometric profile of the samples sintered at 10 °C min^{-1}

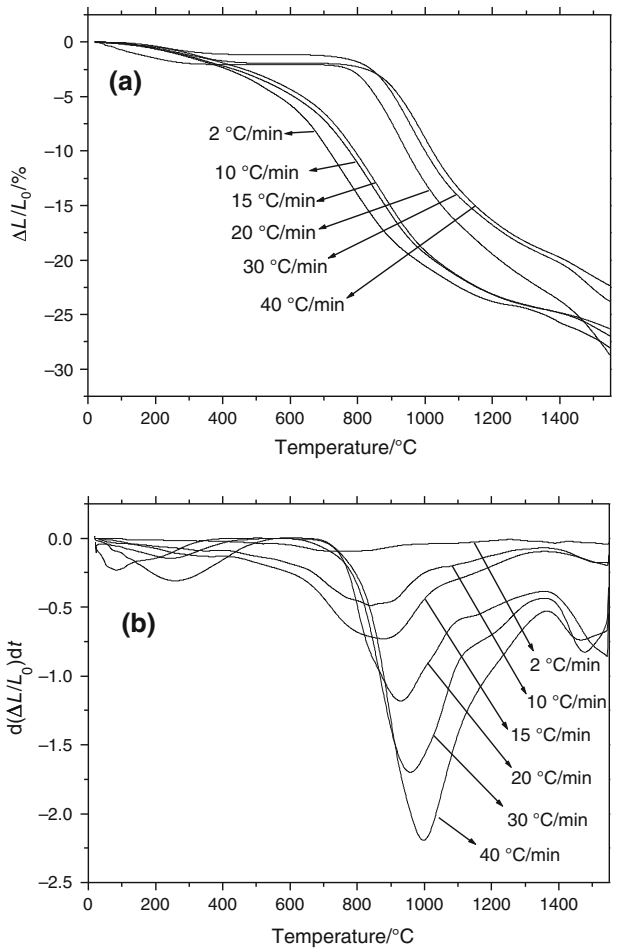

Fig. 2 **a** Dilatometric *curves* obtained at different heating rates and **b** $d(\Delta L/L_0)/dt \times T$

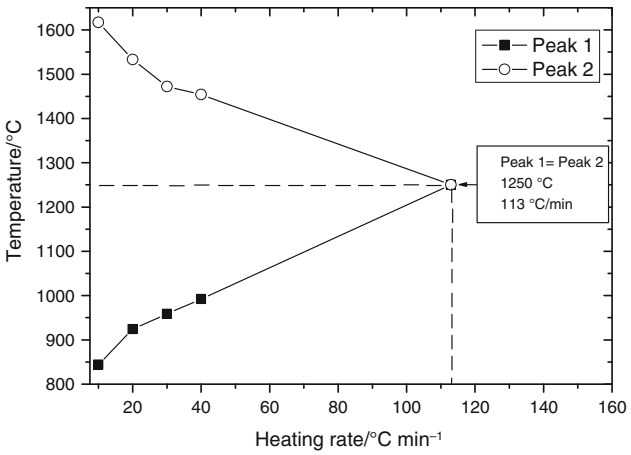

Fig. 3 Temperature of maximum linear shrinkage rate (T^*) as a function of heating rate for both peaks, P_1 and P_2

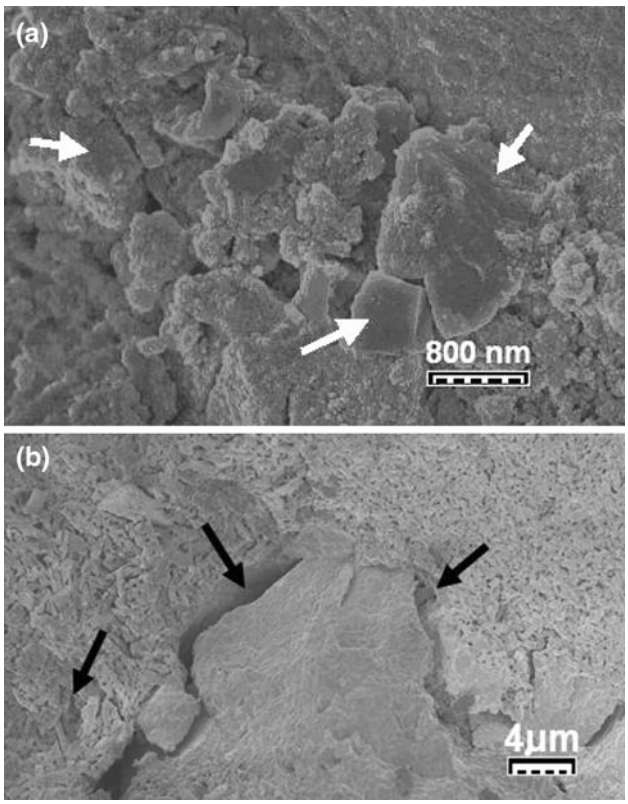

Fig. 4 **a** Image of SEM-FEG green body isostatic pressed and **b** sinterized of 1,450 °C/3 h with 10 °C min^{-1}

The coexistence of two sintering mechanisms associated with the state of nanoparticle agglomeration led us to assume the existence of a single heating rate at which these mechanisms were fully superposed. This hypothetical rate was estimated by extrapolating the temperature of the maximum linear shrinkage rate (T^*) as a function of the heating rate for both peaks, P_1 and P_2 curve, as depicted in Fig. 3. This hypothetical rate was found to be 113 °C min^{-1}, implying an expected sintering temperature of 1,250 °C, which is significantly lower than the reported sintering temperatures of CeO_2 (1,450–1,650 °C [23, 28, 29]). This is not a practical heating rate for conventional furnaces, but is attainable in a microwave-assisted heating device such as a SiC plate. This option is interesting, since the sample is also heated by thermal conduction from the heated SiC plate, as described in the "Experimental" section. To the best of our knowledge, the direct heating of $Ce_{0.85}Gd_{0.15}O_{2-\delta}$ is negligible compared with the heating of a SiC susceptor [30]. In CeO_2 synthesis, microwaves are known to affect the formation of the material, albeit only in a precursor solution. In as-formed material, the expected interaction is vibrational heating, also known as dielectric heating, in which electric dipoles in these materials respond to the applied electric field [31]. In addition, doping with rare-earth ions such as Gd^{3+} and Sm^{3+} reportedly increases the heating efficiency [32].

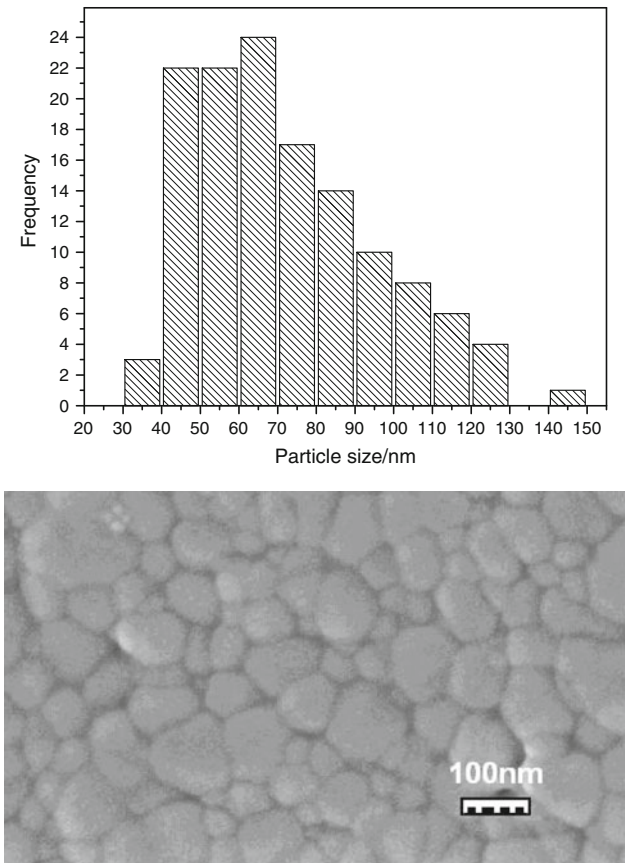

Fig. 5 *Histogram* of the distribution of the particles size and SEM-FEG *image* of samples sintered at 113 °C min^{-1}

Both the method of synthesization and the conformation of the particles led to areas of agglomerated powder, as illustrated in the SEM image of Fig. 4a. These nanometric powder agglomerates (indicated by white arrows) displayed a strong tendency for rapid sinterization at lower temperatures than nonagglomerated particles due to their more numerous contact points, leading to a solid diffusion process. This assumption is illustrated clearly in Fig. 4b, which shows the material treated 1,450 °C/3 h in electric furnace, indicating a grain distribution very similar to that observed in a green sample. This observation is directly correlated to the existence of the two aforementioned sintering mechanisms.

The coexistence of these mechanisms is deleterious to the final properties of the material, leading to the formation of pores and defects, as indicated in Fig. 4b (black arrows). However, as previously postulated, very high-heating rates can favor the simultaneous occurrence of these sintering mechanisms, thereby preventing the occurrence of defects. In fact, as Fig. 5a shows, sintering the samples in microwave oven (heating rate of 113 °C min^{-1}, 1,250 °C during 1 h) resulted in a homogeneous grain distribution ranging from 30 to 150 nm, illustrated in Fig. 5b. Surprisingly, the final densities of the sintered bodies were very high, i.e., 98 %, despite the low density of the green bodies (54 %). This outcome is also a good indication of the effectiveness of this study, specially when comparing the resultant density to obtained by sintering the samples in electric furnace (heating rate of 20 °C min^{-1}, 1,450 °C during 3 h), that results in maximum density of 91 % of the theoretical.

Conclusions

In summary, the very high-heating rates applied here provided an effective way to obtain highly dense, well sintered bodies, despite the presence of agglomerated and nonagglomerated particles in the precursor powders. The simultaneous occurrence of sintering mechanisms also implied a reduction of the sintering temperature. This study is expected to contribute to the ongoing efforts to obtain highly dense ceramic products from nanometric particles, opening up new possibilities for the application of nanostructured materials produced by synthesization in conventional ceramic processes.

Acknowledgements The financial backing of FAPESP and CNPq (both Brazilian agencies) is gratefully acknowledged. The helpful contribution from Mr. Rorivaldo de Camargo in SEM characterization is also acknowledged.

References

1. Kleinlogel C, Gauckler LJ. Sintering and properties of nanosized ceria solid solutions. Solid State Ion. 2000;135:567–73.
2. Steele BCH. Oxygen-transport and exchange in oxide ceramics. J Power Sources. 1994;49:1–14.
3. Ormerod RM. Solid oxide fuel cells. Chem Soc Rev. 2003;32:17–28.
4. Yoshida Y, Arai Y, Kado S, Kunimori K, Tomishige K. Direct synthesis of organic carbonates from the reaction of CO_2 with methanol and ethanol over CeO_2 catalysts. Catal Today. 2006;115:95–101.
5. Yokokawa H, Sakai N, Horita T, Yamaji K, Brito ME. Electrolytes for solid-oxide fuel cells. MRS Bull. 2005;30:591–5.
6. Herring C. Effect of change of scale on sintering phenomena. J Appl Phys. 1950;21:301–3.
7. Camargo ER, Souza FL, Leite ER, Kakihana M. Structural and electrical characterization of dense lead zirconate titanate ceramics synthesized by the oxidant-peroxo wet-chemical route. J Appl Phys. 2004;96:2169–72.
8. Thanneeru R, Patil S, Deshpande S, Seal S. Effect of trivalent rare earth dopants in nanocrystalline ceria coatings for high-temperature oxidation resistance. Acta Mater. 2007;55:3457–66.
9. Goncalves RF, Godinho MJ, Leite ER, Maciel AP, Longo E, Varela JA. Nanocoating of Al_2O_3 additive on ZrO_2 powder and its effect on the sintering behaviour in ZrO_2 ceramic. J Mater Sci. 2007;42:2222–5.
10. Godinho MJ, Goncalves RF, Santos LPS, Varela JA, Longo E, Leite ER. Room temperature co-precipitation of nanocrystalline CeO_2 and $Ce_{0.8}Gd_{0.2}O_{1.9-delta}$ powder. Mater Lett. 2007;61:1904–7.

11. Muccillo ENS, Rocha RA, Tadokoro SK, Rey JFQ, Muccillo R, Steil MC. Electrical conductivity of CeO_2 prepared from nanosized powders. J Electroceram. 2004;13:609–12.
12. Li JG, Ikegami T, Wang YR, Mori T. 10-mol%-Gd_2O_3-doped CeO_2 solid solutions via carbonate coprecipitation: a comparative study. J Am Ceram Soc. 2003;86:915–21.
13. Li JG, Ikegami T, Mori T. Low temperature processing of dense samarium-doped CeO_2 ceramics: sintering and grain growth behaviors. Acta Mater. 2004;52:2221–8.
14. Santos LPS, Longo E, Leite ER, Camargo ER. Combined wet-chemical process to synthesize 65PMN-35PT nanosized powders. J Alloy Compd. 2004;372:111–5.
15. Ribeiro C, Lee EJH, Giraldi TR, Longo E, Varela JA, Leite ER. Study of synthesis variables in the nanocrystal growth behavior of tin oxide processed by controlled hydrolysis. J Phys Chem B. 2004;108:612–5.
16. Kumar KNP, Keizer K, Burggraaf AJ, Okubo T, Nagamoto H, Morooka S. Densification of nanostructured titania assisted by a phase-transformation. Nature. 1992;358:48–51.
17. Bae IJ, Baik S. Abnormal grain growth of alumina. J Am Ceram Soc. 1997;80:1149–56.
18. Ortega FS, Pileggi RG, Studart AR, Pandolfelli VC, Myhre B. IPS, a viscosity-predictive parameter. Am Ceram Soc Bull. 2002;81:44–52.
19. Innocentini MDM, Studart AR, Pileggi RG, Pandolfelli VC. How PSD affects permeability of castables. Am Ceram Soc Bull. 2001;80:31–6.
20. Leite ER, Nobre MAL, Ribeiro MD, Longo E, Varela JA. The effect of heating rate on the sintering of agglomerated $NaNbO_3$ powders. J Mater Sci. 1998;33:4791–5.
21. Harabi A, Belamri D, Karboua N, Mezahi FZ. Sintering of bioceramics using a modified domestic microwave oven. J Therm Anal Calorim. 2011;104:383–8.
22. Nobre MAL, Longo E, Leite ER, Varela JA. Synthesis and sintering of ultra fine $NaNbO_3$ powder by use of polymeric precursors. Mater Lett. 1996;28:215–20.
23. Zhang TS, Ma J, Luo LH, Chan SH. Preparation and properties of dense $Ce_{0.9}Gd_{0.1}O_{2-delta}$ ceramics for use as electrolytes in IT-SOFCs. J Alloy Compd. 2006;422:46–52.
24. de Florio D, Esposito V, Traversa E, Muccillo R, Fonseca F. Master sintering curve for Gd-doped CeO_2 solid electrolytes. J Therm Anal Calorim. 2009;97:143–7.
25. Kingery WD, Berg M. Study of the initial stages of sintering solids by viscous flow, evaporation–condensation, and self-diffusion. J Appl Phys. 1955;26:1205–12.
26. Martin TP, Naher U, Schaber H, Zimmermann U. Evidence for a size-dependent melting of sodium clusters. J Chem Phys. 1994;100:2322–4.
27. Alivisatos AP. Perspectives on the physical chemistry of semiconductor nanocrystals. J Phys Chem. 1996;100:226–39.
28. Rocha RA, Muccillo ENS. Physical and chemical properties of nanosized powders of gadolinia-doped ceria prepared by the cation complexation technique. Mater Res Bull. 2003;38:1979–86.
29. Ishida T, Iguchi F, Sato K, Hashida T, Yugami H. Fracture properties of $(CeO_2)_{(1-x)}(RO_{1.5})_{(x)}$ (R = Y, Gd and Sm; x = 0.02–0.20) ceramics. Solid State Ion. 2005;176:2417–21.
30. Lasri J, Ramesh PD, Schachter L. Energy conversion during microwave sintering of a multiphase ceramic surrounded by a susceptor. J Am Ceram Soc. 2000;83:1465–8.
31. Liao XH, Zhu JM, Zhu JJ, Xu JZ, Chen HY. Preparation of monodispersed nanocrystalline CeO_2 powders by microwave irradiation. Chem Commun. 2001;10:937–8.
32. Santha NL, Sebastian MT, Mohanan P, Alford NM, Sarma K, Pullar RC, Kamba S, Pashkin A, Samukhina P, Petzelt J. Effect of doping on the dielectric properties of cerium oxide in the microwave and far-infrared frequency range. J Am Ceram Soc. 2004;87:1233–7.